Published in final edited form as:
J Immunol. 2013 April 15; 190(8): 4162–4174. doi:10.4049/jimmunol.1202665.

A new model for CD8+ T cell memory inflation based upon a recombinant adenoviral vector[1]

Beatrice Bolinger[*], **Stuart Sims**[*], **Geraldine O'Hara**[*], **Catherine de Lara**[*], **Elma Tchilian**[*], **Sonja Firner**[†], **Daniel Engeler**[†], **Burkhard Ludewig**[†], and **Paul Klenerman**[*,2]

[*]Peter Medawar Building for Pathogen Research, University of Oxford, Oxford, UK [†]Institute of Immunobiology, Cantonal Hospital St. Gallen, CH-9007 St. Gallen, Switzerland

Abstract

CD8$^+$ T cell memory inflation, first described in murine cytomegalovirus (MCMV) infection, is characterized by the accumulation of high-frequency, functional antigen-specific CD8$^+$ T cell pools with an effector-memory phenotype and enrichment in peripheral organs. Although persistence of antigen is considered essential, the rules underpinning memory inflation are still unclear. The MCMV model is, however, complicated by the virus's low-level persistence, and stochastic reactivation. We developed a new model of memory inflation based upon a βgal-recombinant adenovirus vector (Ad-LacZ). After i.v. administration in C57BL/6 mice we observe marked memory inflation in the βgal_{96} epitope, while a second epitope, βgal_{497}, undergoes classical memory formation. The inflationary T cell responses show kinetics, distribution, phenotype and functions similar to those seen in MCMV and are reproduced using alternative routes of administration. Memory inflation in this model is dependent on MHC Class II. As in MCMV, only the inflating epitope showed immunoproteasome-independence. These data define a new model for memory inflation, which is fully replication-independent, internally controlled and reproduces the key immunologic features of the CD8$^+$ T cell response. This model provides insight into the mechanisms responsible for memory inflation, and since it is based on a vaccine vector, also is relevant to novel T cell-inducing vaccines in humans.

Introduction

The induction of potent CD8$^+$ T cell responses is an important goal for vaccine strategies against major pathogens and tumors, and defining the induction and maintenance of CD8$^+$ T cell populations has been the focus of many studies. Many vaccines and natural infections provoke a strong effector memory response in the early phase where the antigen is present but once the non-persistent vector or pathogen is eliminated, CD8$^+$ T cell memory contracts to a "central" memory pool, concentrated in secondary lymphoid organs (1). Much attention has been paid to the situation where antigen is not eliminated and persists at high level, such as in chronic LCMV infection (2, 3). Here CD8$^+$ T cell function is lost over time such that memory is functionally impaired or even lost altogether, a phenomenon known as CD8$^+$ T

[1]The project received support from the Swiss National Science Foundation (PBBSP3-130956 to BB), the Schweizerische Stiftung für Medizinisch-Biologische Stipendien (SSMBS) (PASMP3-134360/1 to BB), the Oxford James Martin School and the Wellcome Trust (WT091663MA).

[2]**Corresponding author and Address**: Prof Paul Klenerman, Peter Medawar Building for Pathogen Research, South Parks Road, Oxford, OX1 3SY, Great Britain. telephone: +44-1865 281885, fax: +44 1865 281236, paul.klenerman@ndm.ox.ac.uk.

[3]Abbreviations used in this paper: Ad-LacZ, βgal-recombinant adenovirus vector; βgal, beta-galactosidase; CD62L, L-Selectin; HBV, Hepatitis B Virus; HCV, Hepatitis C Virus; i.d., intra dermal; LAMP-1, Lysosomal-associated membrane protein 1 (LAMP1) also known as CD107a; LCMV, lymphocytic choriomeningitis virus; LN, lymph node; rAdV, Recombinant adenovirus vector;

Europe PMC Funders Author Manuscripts

cell exhaustion (3). However, exhaustion is not the only outcome of repetitive antigen stimulation. Studies of low level persistent viruses such as CMV have revealed a “mirror image” response to that seen with exhaustion, where T cell responses may be enhanced numerically over time and maintain strong functionality – this has been termed $CD8^+$ T cell memory “inflation” (4). Understanding this phenomenon is relevant not only to disease pathogenesis and the biology of immunologic memory, but also plays a role in vaccine design, where such populations can be harnessed to provide protection against certain chronic viral infections, such as HCV, HIV and CMV (5).

$CD8^+$ T cell memory inflation was first observed in murine CMV (MCMV) infection (4, 6), and similar findings are observed in human CMV (HCMV) infection. In $CD8^+$ T cell memory inflation responses to a single epitope may become very large, and are maintained at high levels throughout life (4, 7, 8). CMV-specific inflating $CD8^+$ T cells typically show an extreme of the “effector-memory” phenotype ($CD27^{lo}$, $CD28^-$, $CD62L^-$, $CD127^{lo}$ and $IL\text{-}2^{+/-}$) (9). Cells remain functional and respond vigorously to viral re-challenge, providing protection (4). They are located in the spleen and the periphery, particularly in organs such as liver and lung. It is unclear yet what drives the selection of these “inflationary” epitopes, but it has been shown that it is independent of initial immunodominance (10) and viral gene-expression patterns (11). In MCMV, for example, only one of two epitopes from the same protein is associated with an “inflationary” response (12, 13). This suggests other factors than the kinetics of the viral gene expression could be involved; in particular recent data reveal immunoproteasome-independence is associated with inflation and suggest a significant role for antigen processing in epitope selection during memory development (14).

However, in the MCMV model many questions remain unanswered. The location and the nature of the cells which process and present antigen and eventually sustain $CD8^+$ T cell responses are still elusive. Likewise, it is not known for how long antigen needs to be presented to produce such a sustained $CD8^+$ T cell response. It appears that repetitive antigen exposure is an essential factor driving memory inflation, as suggested by analysis of phenotype and activation status (4, 10) and adoptive transfer into naïve hosts (9). Recent work has revealed that ongoing production of infectious MCMV is, however, not an absolute requirement (15, 16). Critically, MCMV is a complex model virologically, with a very large genome containing numerous immunoevasins, long term low level persistence and stochastic reactivation at diverse sites. Thus a simpler and more tractable system to investigate these questions would be desirable.

The phenomenon of memory inflation is not exclusive to CMVs as it is also observed in other viral infections (17-20). However, it has not been described after immunization with non-replicating vaccine vectors. Recombinant viral vectors for antigen delivery are key to many novel vaccine strategies. In this field, adenovirus vectors (AdV) have emerged among the most potent of these (21-24). They transduce a variety of cells, but the vector genome does not integrate and their safety is well established (25). Depending on dose, route of immunization and the transgene used, a spectrum of different T cell responses are elicited after immunization with rec-AdV. These responses may range from complete abolition of a functional response to expansion and differentiation of effector T cells (26-31). In the present study, we showed for the first time, that rec-AdV was capable to induce robust, sustained $CD8^+$ T cell memory inflation, which mimics that seen after MCMV infection.

Using a β-galactosidase recombinant adenovirus vector (Ad-LacZ), we found this replication-deficient virus to induce strong memory inflation *in vivo* – independent of viral reactivation. The system has a number of internal controls, including, critically, a non-inflating epitope generated from the same transgene. Using this model, βgal_{96}-specific

$CD8^+$ T cells show memory inflation with up to 20% specific cells on d21, increasing to 30% on d100 in blood, with further enrichment in tissues such as liver and lung. In contrast, responses against the βgal_{497} epitope show classical stable memory with early induction followed by low levels over time. As after MCMV infection, $CD8^+$ T cell memory inflation after Ad-LacZ immunization develops after a single i.v. dose and the induced $CD8^+$ T cells show an identical effector-memory phenotype.

Overall, immunization with Ad-LacZ provides a unique and robust model for memory inflation. It has broader implications not only for examining the basic biology of sustained effector memory populations, but also with direct relevance to vaccine development.

Materials and Methods

Ethics statement

Mouse experiments in Oxford were performed according to UK Home Office regulations (project licence number PPL 30/2235 and 30/2744) and after review and approval by the local ethical review board at the University of Oxford. Experiments in St Gallen were performed in accordance with Swiss Kantonal and federal legislations and were approved by the Veterinary Officer of the Kanton of St Gallen.

Adenoviral vector

Recombinant adenovirus expressing the βgal protein under the control of the human CMV promoter (Ad-LacZ) and lacking E1 and E3 genes was used (28). Ad-LacZ was propagated on permissive HER-911 cells and was purified with the Vivapure AdenoPack 20 (Sartorius, Stedim biotech, 13781 Aubagne Cedex, France) according to the manufacturer's specifications. Virus titer was determined in a cytopathic effect assay. Briefly, serial dilutions of the adenovirus were used to infect HER-911 cells on a 96-well microtiter plate and cytopathic effect was determined after 5 days by microscopy. Tissue culture infectious dose of 50% was calculated by the Reed-Muench method. Ad-LacZ aliquots were stored at −80°C in PBS and injected either intravenously or intradermal (earlobe) at a dose of 2×10^9 pfu.

Viruses

Recombinant MCMV expressing the βgal protein under the transcriptional control of the human CMV *ie*1/*ie*2 promoter-enhancer (MCMV-LacZ RM427 (32)) was used. MCMV-LacZ was propagated and titrated on NIH 3T3 cells (ECACC, UK) and injected intravenously at a dose of 2×10^5 pfu.

Recombinant Vaccina expressing the βgal protein (Vacc-LacZ) (33) was used. VV-LacZ was propagated and titrated on BSC-40 cells and injected i.p. at a dose of 2×10^6 pfu.

Mice

Male and female C57BL/6 mice were obtained from Harlan (UK). MHC II-KO (34) mice were on the C57BL/6 background. TCR transgenic Bg1 mice that express a TCR recognizing the H2-Kb-restricted $\beta\text{-gal}_{96\text{-}103}$ peptide on more than 95% of their $CD8^+$ T cells have been described previously (35). Bg1 mice have been generated by Dr Nicholas P. Restifo, (National Cancer Institute (NCI), Bethesda, MD, USA) and were kindly provided by Dr Chris Norbury (Penn State Milton S. Hershey College of Medicine, Dept. of Microbiology and Immunology, USA) Bg1 mice were crossed with C57BL/6-SJL mice expressing the congenic marker Ly5.1 (CD45.1) kindly provided by Dr Kevin Maloy (Dunn School, University of Oxford, UK). Transgene expression was monitored by staining of blood cells with anti-Vβ7 by flow cytometry. LMP7 knock out mice (36) on the C57BL/6

background were kindly provided by Professor Dr Marcus Groettrup (Division of Immunology, Department of Biology, University of Constance, 78457 Konstanz, Germany). All animals were kept under conventional conditions in individually ventilated cages and fed with normal chow diet. Experiments were carried out with age and sex-matched animals.

Peptides

The $\beta gal_{96\text{-}103}$ (DAPIYTNV) (37), the $\beta gal_{497\text{-}504}$ (ICPMYARV) (38) and the M45 (HGIRNASFI) (39) peptide were purchased from Mimotopes (Victoria, Australia).

Antibodies

Anti-CD8-PerCp-Cy5.5, anti-CD8-eFluor® 450, anti-CD3-Alexa700, anti-TNFα-FITC, anti-IFNγ-eFluor® 450, anti-CD62L-FITC, anti-CD62L-PE-Cy7, anti-CD122-eFluor® 450, anti-CD127-PE-Cy7, anti-CD45.1-eFluor® 450 and anti-NKG2A,B-PE were obtained from ebioscience (San Diego, USA). Anti-NKG2A,C,E-FITC, anti-Vβ7-FITC and anti-CD44-FITC were obtained from BD Bioscience (Oxford, UK), anti-CD44-PE-Cy7, anti-CD107a-APC, anti-NKG2D-FITC and anti-CD27-PerCP-Cy5.5 were obtained from Biolegend (San Diego, USA), anti-KLRG-1-FITC was obtained from Abcam (Cambridge, UK).

Flow cytometry

For flow cytometry, single cell suspensions were generated from the indicated organs and 1×10^6 cells were incubated with the indicated mAb at 4°C for 20 min. For PBL samples, erythrocytes were lysed with FACS Lysing Solution (BD PharMingen). Cells were analyzed by flow cytometry using a BD LSR II flow cytometer and FlowJo software, gated on viable leukocytes using the live/dead fixable near-IR dead cell stain kit from Invitrogen (Paisley, UK).

Isolation of liver and lung lymphocytes

Perfused livers were smashed through a cell strainer (BD) and lymphocytes were purified by a Percoll (GE healthcare) gradient centrifugation. Lungs were minced with razor blades and incubated in phosphate-buffered saline (PBS) containing 60U/ml DNase (AppliChem) and 170U/ml collagenase II (Gibco) at 37°C for 45 min. Cell aggregates were dispersed by passing the digest through a cell strainer (BD).

Intracellular cytokine staining

Spleens, livers and lungs were removed at indicated timepoints after immunization with 2×10^9 pfu Adeno-LacZ. Single cell suspensions of 2×10^6 lymphocytes were incubated for 2h at 37°C in 150 μl of culture medium (RPMI) containing 5% FCS in 96-well round-bottom plates. The cells were stimulated with phorbol myristate acetate (PMA) (50 ng/ml) and ionomycin (500 ng/ml) as a positive control or left untreated as a negative control. Peptide-specific responses were analyzed after cells were stimulated with 10^{-6} M $\beta gal_{96\text{-}103}$ (DAPIYTNV) or $\beta gal_{497\text{-}504}$ (ICPMYARV) peptide (both from Mimotopes (Victoria, Australia)). After 2h stimulation at 37°C, 50μl GolgiPlug (1μl/1ml final concentration) from BD Bioscience (Oxford, UK) was added and cells were incubated for another 4h at 37°C. Cells were fixed with the cytofix/cytoperm solution from BD Bioscience (Oxford, UK) and stained and washed with Perm/Wash buffer from BD Bioscience (Oxford, UK). $CD8^+$ T cells producing IFNγ, TNFα or LAMP-1 were determined using a BD LSR II flow cytometer and FlowJo software.

Construction of tetrameric MHC class I peptide complexes

MHC class I monomers complexed with βgal (H-2Kb) were produced as previously described (40) and tetramerized by addition of streptavidin-PE (BD Biosciene, Oxford, UK)

or streptavidin-APC (Invitrogen, Paisley, UK). At the indicated time points following infection, organs were removed and single cell suspensions were prepared. Aliquots of 1×10^6 cells or 100 μL of blood were stained using 50 μL of a solution containing tetrameric class I-peptide complexes at 37°C for 20 min followed by staining with mAbs at 4°C for 20 min. Absolute cell counts were determined by counting leukocytes in an improved Neubauer chamber.

In vivo cytotoxicity

Single cell suspensions from spleens of C57BL/6 mice were subjected to hypotonic red blood cell lysis. Before injection, half of the cells were loaded with 10^{-5} M $\beta gal_{96\text{-}103}$ peptide and stained with CellTrace violet (Invitrogen, Paisley, UK). A maximum concentration of 5×10^6 cells/mL were incubated in 5 μM CellTrace violet in PBS or in 0.5 μM CellTrace violet (negative population) for 20 minutes at 37°C. Cells were washed and resuspended in PBS at a concentration of 5×10^7 splenocytes/mL each group. Recipient B6 mice were injected intravenously with 10×10^7 splenocytes in 200 μL PBS. 12h later, blood, spleen, liver and lungs were harvested and single cell suspension generated. Cells were analyzed by flow cytometry using a BD LSR II flow cytometer and FlowJo software and gated on viable leukocytes using the live/dead fixable near-IR dead cell stain kit from Invitrogen (Paisley, UK).

The ratio of killed cells to control cells was calculated to obtain the % of specific killing.

Extraction and quantification of LacZ genome copy numbers in tissue

Tissues were homogenized using a MagNA Lyser instrument (Roche Diagnostics). Whole DNA was isolated using the High Pure PCR Template Preparation Kit (Roche Diagnostics). Real-time quantitative PCR was performed using a Light cycler 480 Real-Time PCR System (Roche Diagnostics) and the LightCycler 480 probes master reaction mix (Roche Diagnostics) according to the manufacturer's protocol. Data analysis was performed with LightCycler 480 Software (Roche Diagnostics). Oligonucleotides were purchased from Eurofins MWG Operon (Ebersberg, Germany). The following oligonucleotides from LacZ protein sequences were used as primers for real-time quantitative PCR: 5′-GCGTGGATGAAGACCAGC-3′ and 5′ CGA AGC CGC CCT GTA AAC 3′. The following oligonucleotides were used as probes: 5′ CAG TCT TGG CGG TTT CGC TAA 3′ and 5′ TAC TGG CAG GCG TTT CGT CAG 3′. Probe 1 carried a 3′ FAM reporter and probe 2 was Cy5 labeled at the 5′ end. Thermal cycling started with HotStarTaq activation during 15 min at 95°C. Thereafter 50 cycles of amplification were run consisting of 15 s at 95°C, 20 s 60°C, and 20 s of 72°C. A negative control, containing reagents only, and serial dilutions of plasmid containing the specific LacZ sequence were included in each run to generate a standard curve. The concentrations of the plasmid dilutions were: 280000, 28000, 2800, 280, and 28 copies per reaction. LacZ DNA concentration in the unknown samples was calculated using the data from the standard curve. Each sample was measured as triplicates and the average concentration was used for calculation. Final copy numbers per μg DNA were calculated.

Extraction of RNA and of LacZ-specific mRNA by quantitative real-time PCR

Organs were homogenized in Trizol (Sigma-Aldrich, USA) using a MagNA Lyser instrument (Roche Diagnostics). RNA was isolated by isopropanol percipitation, washed with ethanol 70% and resuspended in DEPC-water. RNA was DNAse treated with DNAse I (Invitrogen, Paisley, UK) and subjected to RT-PCR using 2μg purified RNA. For RT-PCR the high capacity cDNA archive Kit from Applied Biosystem (ABI PRISM, Warrington, United Kingdom) was used according to the specifications of the manufacturer to generate cDNA from RNA samples. Quantitative real-time PCR was performed using a Light cycler

480 Real-Time PCR System (Roche Diagnostics) and the LightCycler 480 probes master reaction mix (Roche Diagnostics) following the manufacturer's protocol. Data analysis was performed with LightCycler 480 Software (Roche Diagnostics). Oligonucleotides were purchased from Eurofins MWG Operon (Ebersberg, Germany). The following oligonucleotides from LacZ sequences were used as primers for quantitative real-time PCR: 5′-GCGTGGATGAAGACCAGC-3′ and 5′-CGAAGCCGCCCTGTAAAC-3′. The following oligonucleotides were used as probes: 5′ CAGTCTTGGCGGTTTCGCTAA 3′ (probe 1) and 5′ TACTGGCAGGCGTTTCGTCAG 3′ (probe 2). Probe 1 carried a 3′ FAM reporter and probe 2 was Cy5 labeled at the 5′ end. Thermal cycling started with HotStarTaq activation during 15 min at 95°C. Thereafter 50 cycles of amplification were run consisting of 15 s at 95°C, 20 s 60°C, and 20 s of 72°C. A negative control, containing reagents only, and serial dilutions of plasmid containing the specific LacZ sequence were included in each run to generate a standard curve. The concentrations of the plasmid dilutions were: 280000, 28000, 2800, 280, and 28 copies per reaction. LacZ mRNA concentration in the unknown samples was calculated using the data from the standard curve. Each sample was measured as a triplicate and the average concentration was used. Final copy numbers were calculated per μg total RNA.

Adoptive transfer of TCR transgenic T cells

Single cell suspensions from spleens of Ly5.1$^+$ Bg1 mice were subjected to hypotonic red blood cell lysis and stained with CFSE (Invitrogen, Paisley, UK). A maximum concentration of 2.5×10^7 cells/mL were incubated in 5 μM CFSE in PBS for 10 minutes at 37°C. Cells were washed twice with ice-cold PBS and resuspended in PBS at a concentration of 1×10^7 splenocytes/mL. Recipient B6 mice were injected intravenously with 2×10^6 Bg1-Ly5.1$^+$ splenocytes in 200μL PBS.

Statistical analysis

To evaluate statistically significant differences, the unpaired two-tailed Student's test was used. *p* values smaller than 0.05 were considered statistically significant. Statistical data analysis was performed using Graph-Pad Prism version 5.0a for MACs (GraphPad Software, San Diego, CA, USA).

Results

Epitope-specific CD8$^+$ T cell memory inflation following adenovirus vector immunization

Immunization of C57BL/6 mice with the replication-deficient Ad-LacZ induced a strong CD8$^+$ T cell response in blood on day 21 against two distinct βgal epitopes (βgal_{497} and βgal_{96}). On day 300, βgal_{497}-specific CD8$^+$ T cells had contracted and were detectable at low levels only, while the βgal_{96}-specific CD8$^+$ T cell population had increased further (Figure 1A).

In order to better define the kinetics of the βgal-specific CD8$^+$ T cell responses induced by Ad-LacZ, C57BL/6 mice were inoculated i.v. with a single dose of Ad-LacZ and tracked longitudinally. Lymphocytes from blood, spleen, liver, lung, and lymph nodes (LNs) were isolated at different timepoints and βgal-specific CD8$^+$ T cells quantified by staining with MHC class I tetramers. βgal_{96}-specific CD8$^+$ T cells showed memory inflation with up to 20% specific cells on day 21, followed by a continued increase over time to 30% on day 100 in blood (Figure 1B). These cells were further enriched in tissues such as spleen, liver and lung on day 100 (Figure 1C). As in blood, in these organs the βgal_{96}-specific CD8$^+$ T cell population was maintained over time (Figure 1D).

In contrast to βgal_{96}-specific $CD8^+$ T cells, tetramer staining for βgal_{497}-specific $CD8^+$ T cells revealed only low levels of tetramer-positive $CD8^+$ T cells on day 100 in spleen, liver and lung (Figure 1C). The initial expansion phase was followed by contraction and classical stable memory at low but detectable levels over time (Figure 1D). When data were displayed as absolute numbers of antigen-specific T cells per organs, comparable results were obtained (Figure 1E). On day 200 the total amount of βgal_{96}-specific $CD8^+$ T cells in spleen and liver was more than 25 times higher than the amount of βgal_{497}-specific $CD8^+$ T cells whereas in the lung it was 50 times more, the latter two, indicating a major redistribution of βgal_{96}-specific $CD8^+$ T cells to peripheral organs.

Only low frequencies of βgal_{96} and βgal_{497}-specific $CD8^+$ T cells were found in LNs (inguinal LN) (βgal_{96}-specific $CD8^+$ T cells: d21=0.6±0.1%, d50=0.4±0.1%, d100=0.4±0.1%,; βgal_{497}-specific $CD8^+$ T cells: d21=0.3±0.1%, d50=0.09±0.03%, d100=0.02±0.01%,), where βgal_{96}-specific $CD8^+$ T cells did not inflate, as observed in MCMV infection (10, 41).

$CD8^+$T cell memory inflation is not restricted to the i.v. route, but is confined to the vector

It has been shown previously that the localization of the inoculum of adenovirus vectors determines the quality of $CD8^+$ T cell responses (26). Thus, to identify whether memory inflation in the Ad-LacZ model is restricted to the i.v. route we evaluated the βgal-specific $CD8^+$ T cell response following i.v. and intradermal (i.d.) Ad-LacZ injection in blood of C57BL/6 mice. We performed tetramer staining for the inflating (βgal_{96}) and the non-inflating epitope (βgal_{497}) (Figure 2A). Interestingly, exactly the same pattern for both the βgal_{96}- and βgal_{497}-specific $CD8^+$ T cell response is seen after i.v. and i.d. immunization. Although, the βgal_{96}-specific response was significantly reduced after i.d. immunization compared to i.v., $CD8^+$ T cell maintenance was not impaired, and βgal_{96}-specific $CD8^+$ T cells clearly showed memory inflation in this setting. This is even better illustrated looking at the inflationary potential of the $CD8^+$ T cell responses, by considering the day 100 to day 21 ratio of tetramer-positive cells (Figure 2B). This ratio is used to distinguish responses where there is a strong contraction detectable in blood after the day 21 peak to those where there is maintenance and/or expansion over time. Here, compared to βgal_{497}-specific $CD8^+$ T cells, which do not inflate, βgal_{96}-specific $CD8^+$ T cells, after both, i.v. and i.d. immunization, show a ratio higher than 1, indicating that these cells are maintained over time and $CD8^+$ T cell memory inflation after Ad-LacZ is not restricted to the i.v. route.

We further assessed whether βgal-specific $CD8^+$ T cell memory inflation is confined to Ad-LacZ. Therefore, we infected C57BL/6 mice with a βgal-recombinant MCMV (MCMV-LacZ) or Vaccinia (Vacc-LacZ). MCMV-LacZ and Vacc-LacZ infection induced a very small but significant βgal_{497}-specific $CD8^+$ T cell response in blood, compared to non-immunized (naïve) mice (p-value MCMV-LacZ d7 compared to background in naïve mice = 0.0238; p-value Vacc-LacZ d7 compared to background in naïve mice = 0.0392). The βgal_{96}-specific $CD8^+$ T cell response was detected but at levels not significantly above background (Background in naïve mice: 0.17%±0.02; d7 MCMV-LacZ: 0.4%±0.07; d7 Vacc-LacZ: 0.31%±0.08)(Figure 2E). Taken together these data revealed that if the transgene was expressed in a different vector, although a βgal_{497}-specific $CD8^+$ T cell was primed, no $CD8^+$ T cell memory inflation was induced (Figure 2 C,D), indicating that the latter is not solely a property of the insert.

Overall, our data suggest that antigen presentation established after both i.v. and i.d. inoculation is sufficient to maintain inflationary responses and βgal-specific $CD8^+$ T cell memory inflation is exclusive to the adenovirus vector.

Progressive expansion of effector memory CD8$^+$ T cells

To further characterize βgal$_{96}$-specific CD8$^+$ T cells generated after i.v. inoculation, we compared them with MCMV-specific inflationary CD8$^+$ T cells, using phenotypic markers defined from conventional analyses of MCMV-specific cells (4, 9, 10). Hence, we co-stained βgal-tetramer$^+$ CD8$^+$ T cells for adhesion and trafficking molecules such as CD44 and CD62L, for the cytokine receptor CD127 (IL-7Rα), the NK-cell receptors KLRG-1, NKG2A and D and the co-stimulatory marker CD27 and compared them to the tetramer-negative CD8$^+$ T cell population (Figure 3A; Supplementary Figure 1A,B). Staining for CD44 and CD62L indicated that inflating cells are a memory pool with a predisposition to accumulate in non-lymphoid organs (CD44^{hi} CD62L^{lo}). The inflating population down regulated IL-7Rα, expressed IL-15Rβ, was high in KLRG1, NKG2A and D and showed reduced expression of the co-stimulatory molecule CD27 compared to tetramer$^-$ CD8$^+$ T cells. These characteristics are typical for an antigen-experienced effector-memory CD8$^+$ T cell population.

We next examined the expression of these markers on βgal$_{96}$-specific inflationary CD8$^+$ T cells, βgal$_{497}$-specific and total CD8$^+$ T cells in blood, spleen, liver and lung up to day 200 after immunization (Figure 3B; Supplementary Figure 1C-F). We demonstrated that βgal$_{96}$-specific inflationary CD8$^+$ T cells barely changed their phenotype over time. They display a comparable effector-memory phenotype (CD62L^{lo}, CD27^{lo}, IL-7R^{lo}, KLRG-1^{hi}, NKG2A/D^{hi}) from day 21, which is maintained up to day 200 after immunization.

In contrast to these data, βgal$_{497}$-specific CD8$^+$ T cells acquired a divergent phenotype after contraction. This had features of a central memory pool (CD62l^{hi}, CD27^{hi}, IL-7R^{hi} and KLRG1^{lo}) especially in the spleen and blood. They were also low in expression on NKG2D and NKG2A (Figure 3B; Supplementary Figure 1C-F).

Importantly, βgal$_{96}$-specific CD8$^+$ T cells after i.d. injection, displayed an identical effector-memory phenotype on day 21, 50 and 100 in blood as that seen after i.v. immunization (Supplementary Figure 2C).

We also went on to test the impact of inoculation on induction of memory and phenotype via alternative routes such as subcutaneous (s.c.) and intramuscular (i.m.). We noted that βgal$_{96}$-specific CD8$^+$ T cells do not inflate numerically after s.c injection of Ad-LacZ, although a distinction between the kinetics of the βgal$_{96}$-specific CD8$^+$ T cells, and βgal$_{497}$-specific CD8$^+$ T cells could still be observed. However, the generation of the effector memory phenotype associated with the βgal$_{96}$-specific CD8$^+$ T cells was clear in all cases and independent of the route of immunization (Supplementary Figure 2).

Taken together, Ad-LacZ induced two completely distinct CD8$^+$ T cell memory populations: the conventional (βgal$_{497}$-specific CD8$^+$ T cell) population with a T_{CM} phenotype and the inflationary (βgal$_{96}$-specific CD8$^+$ T cell) population, with progression towards an effector-memory phenotype, identical to that seen in MCMV infection (4, 9, 10, 16, 41) and independent of the route of injection. Interestingly, this is true for lymphocytes from blood, spleen, liver and lung but not from LNs. In LNs, the fraction of βgal$_{96}$-specific cells, which displayed a central-memory phenotype (T_{CM}), was much higher, with more than 30% (data not shown). This impact through the anatomical site was also reported after MCMV infection (10, 41).

βgal$_{96}$-specific CD8$^+$ T cells retain functionality and show rapid acquisition and maintenance of cytotoxicity

We next assessed the functionality of the “inflating” memory population. Intracellular staining for IFNγ and TNFα following peptide stimulation revealed that inflationary βgal-

specific $CD8^+$ T cells efficiently secreted effector cytokines (Figure 4 and 5A,B). Indeed, both sets of βgal-specific memory cells are strong IFNγ and TNFα producers upon stimulation with the cognate peptide. Whereas IFNγ and TNFα secretion on day 21 is comparable for both βgal-specific populations, inflationary $CD8^+$ T cells, especially in peripheral organs, dominated cytokine secretion in the memory phase (Figure 4, 5A,B).

Furthermore, staining for IFNγ, TNFα and LAMP-1 revealed that βgal_{96}-specific inflationary $CD8^+$ T cells were polyfunctional. On day 100 post immunization, most of the $IFN\gamma^+$ $CD8^+$ T cells in spleen, liver and lung were also positive for LAMP-1, indicating that they had degranulated and released effector molecules. Many IFNγ-producing, LAMP-1-positive inflationary $CD8^+$ T cells additionally secreted TNFα. This pattern of functionality was seen at all timepoints measured (Figure 5A,B). Overall, if we consider the difference in the amount of βgal_{96}- and βgal_{497}-specific $CD8^+$ T cells, calculating the ratio of IFNγ- or TNFα-producing cells to tetramer-positive cells, although both populations are clearly functional, βgal_{497}-specific $CD8^+$ T cells are stronger IFNγ and TNFα producers on a per-cell basis (data not shown). Furthermore, this ratio also revealed a higher number of IFNγ- and TNFα-producing $CD8^+$ T cells compared to βgal_{497}-specific $CD8^+$ T cells after stimulation with βgal_{497-} peptide. We suggest that the βgal_{497}-tetramer may bind specific T cells with a relatively low avidity, hence the frequency of tetramer-specific $CD8^+$ T cells might be underestimated compared to the true frequency. Alternatively there may be binding to distinct MHC molecules. Both alternatives will be assessed further in future studies.

We next assessed the killing capacity of the βgal-specific $CD8^+$ T cells, using an in vivo cytotoxicity assay. βgal_{96}-peptide-pulsed target cells were efficiently killed in vivo 12 hours after adoptive transfer into day 21, day 50 and day 100 immune mice. This is seen not only in spleen and blood (Figure 5C) but also in peripheral organs such as liver and lung (Figure 5D) at all timepoints, indicating that inflationary $CD8^+$ T cells retain their cytotoxic capacity. In comparison, βgal_{497}-peptide-pulsed target cells, were killed in a much lower degree, especially if transferred into day 100 mice.

Overall, although βgal_{96}-specific $CD8^+$ T cells show evidence of repeated antigen exposure, they are not exhausted and remain functional, even at day 100 after immunization.

Low-level antigen persistence enables $CD8^+$ T cell memory inflation

Compared to MCMV infection, the Ad-LacZ model is virologically simple. There is no viral replication, which clearly facilitates tracking the virus, and both epitopes are generated from a single gene product.

In order to establish whether viral genome persists, we performed quantitative realtime PCR. LacZ DNA copy numbers per microgram total DNA were assessed in spleen, liver, lung and hepatic LNs (hLN) at different timepoints after Ad-LacZ immunization. On day 300, viral genome was still found in spleen, liver and lung, but not in hepatic LNs (Figure 6A).

Next, we addressed whether the transgene was still expressed at late timepoints. To do this, first, quantitative real-time PCR for LacZ mRNA was performed. LacZ mRNA could only be quantified in liver and draining LNs (hLNs) around day 2 after immunization; thereafter, only low levels of specific mRNA was detected, but below the level of quantification (Figure 6B).

Although, antigen was not detectable on the RNA level, the effector phenotype of inflationary memory T cells strongly suggests continuous transgene exposure, most likely through low-level antigen expression. To test this we adoptively transferred CFSE labeled βgal_{96}-specific TCR transgenic $CD8^+$ T cells from Bg1 mice into naïve C57BL/6 mice and

day 20, day 50 and day 100 immune recipients. Three days later, proliferation and activation of transferred cells was measured in spleen, liver, hLNs and lung by staining for CD44 and quantifying CFSE dilution by FACs analysis. While, antigen expression could not be readily detected at day 20 post immunization at the transcriptional level, TCR transgenic $CD8^+$ T cells vigorously proliferated when transferred into day 20 mice (Figure 6C,D). Even in day 50 and day 100 immune mice adoptively transferred cells became activated and proliferated, though in a lesser extent (Supplementary Figure 3A). The percentage of proliferated TCR transgenic cells was comparable in day 4, 8 and 14 immune mice. In day 20 immune mice proliferation was slightly reduced compared to the previous days and it was further reduced in day 50 and day 100 immune mice (Figure 6D).

Taken together, these results demonstrate that $CD8^+$ T cell memory inflation in this setting is not dependent on viral reactivation and replication; similar findings have been reported for MCMV infection (15, 16).

To assess whether the absence of a βgal_{96}-specific inflating response after MCMV-LacZ or Vacc-LacZ infection was due to the lack of antigen presentation, we likewise adoptively transferred CFSE labeled βgal_{96}-specific TCR transgenic $CD8^+$ T cells from Bg1 mice into day 100 MCMV-LacZ immune and day 21 Vacc-LacZ immune recipients, respectively. In MCMV-LacZ immune recipients adoptively transferred cells became activated and proliferated compared to naïve recipients (Supplementary Figure 3B). In Vacc-LacZ immune recipients in contrast, adoptively transferred cells did not proliferate compared to naïve recipients (Supplementary Figure 3C). These results together with data from Figure 2C and D suggest that Vacc-LacZ is efficiently cleared on day 21 after infection, hence no memory inflation is observed. However, after MCMV-LacZ infection the βgal_{96} epitope was still presented on day 100 after infection, suggesting factors other than pure antigen availability are responsible for the lack of $CD8^+$ T cell memory inflation after MCMV-LacZ infection.

$CD4^+$ T cell help facilitates inflation of memory effector T cells

To further explore the critical requirements for $CD8^+$ T cell memory inflation using this model, we investigated the role of $CD4^+$ T cell help. $CD4^+$ T cells are essential for $CD8^+$ T cell memory induction across a range of immunizations, (42) and acute infections (43, 44), although their role in memory inflation after MCMV infection is not fully defined (16, 45).

To establish the role of $CD4^+$ T cells in memory inflation after i.v. Ad-LacZ immunization, we assessed the βgal_{96}-specific $CD8^+$ T cell response on different timepoints in blood of MHC-II deficient and wild-type (WT) C57BL/6 mice. In this setting, the generation of tetramer-positive $CD8^+$ T cells was clearly dependent on $CD4^+$ T cell help. Only low levels of βgal_{96}-specific $CD8^+$ T cells could be detected on day 21, 50 and 100 after immunization and the percentage in MHC-II-KO mice was significantly reduced at all timepoints, compared to C57BL/6 mice (Figure 7A). Staining for βgal_{96}-specific $CD8^+$ T cells in spleen, liver and lung on day 100 revealed similar results, with the tetramer-positive population significantly reduced in MHC-II-KO mice compared to WT mice (Figure 7B).

The fact that βgal_{96}-specific $CD8^+$ T cells developed in MHC-II-KO mice and were maintained up to day 100 suggests a $CD4^+$ T cell independency for the $CD8^+$ T cell maintenance. This was further confirmed looking at their inflationary potential in blood with a day 100 to day 21 ratio higher than 1, as seen in the WT mice (Figure 7C). Staining βgal_{96}-specific $CD8^+$ T cells from blood, spleen, liver and lung for phenotypic markers (on day 100), βgal_{96}-specific $CD8^+$ memory T cells from MHC-II-KO mice showed a T_{CM} phenotype (IL-$7R^{hi}$, $CD62L^{hi}$, KLRG-1^{lo}, $CD27^{hi}$) compared to the T_{EM} phenotype seen in C57BL/6 mice. This T_{CM} phenotype directly developed after day 21 (data not shown).

Overall these results show that not only $CD8^+$ T cell priming and late expansion but also $CD8^+$ T cell phenotype in this system is $CD4^+$ T cell help dependent. Mechanisms independent of $CD4^+$ T cell help may provide limited signals for maintenance of the residual memory pools.

βgal_{96}-specific $CD8^+$ T cell memory inflation is immunoproteasome-independent

To address antigen presentation in this setting, we assessed whether βgal-epitopes are processed via immunoproteasomes or via constitutively expressed proteasomes using LMP-7-KO mice. These mice have a deletion of the gene encoding LMP-7, a subunit of the immunoproteasome encoded in a region of the major histocompatibility complex (MHC) that is critical for class I-restricted antigen presentation (36). LMP-7 functions as an integral part of the peptide supply machinery and consequently, LMP-7-KO mice are not able to process antigen via immunoproteasomes. Immunizing LMP-7-KO mice with Ad-LacZ induced a strong βgal_{96}-specific $CD8^+$ T cell response on day 21 in blood, which is comparable to the one seen in WT animals. The βgal_{96}-specific $CD8^+$ T cell populations expanded further with up to 30% of tetramer-positive cells on day 100, which was again equivalent to the tetramer-positive response seen in C57BL/6 mice (Figure 7D,E).

In contrast, βgal_{497}-specific $CD8^+$ T cells showed only 0.4% tetramer-positive cells on day 21 in blood compared to 7.7% in WT mice. Not only was the expansion of these cells significantly reduced, but also the memory population, with only very low levels of specific $CD8^+$ T cells on day 50 and 100 (Figure 7F,G).

These findings clearly demonstrate that processing of the βgal_{497} epitope is immunoproteasome-dependent, whereas that of βgal_{96} and therefore memory inflation, in this setting, is not. These features may contribute to the different outcome of the two βgal-specific $CD8^+$ T cell responses after Ad-LacZ immunization.

Discussion

The main characteristics of $CD8^+$ T cell memory inflation, largely known from studies with MCMV, are 1) inflating $CD8^+$ T cell populations increase and are maintained at a very high frequency over time; 2) they show an effector memory phenotype and they are distributed in peripheral organs, such as liver or lung and 3) although they show features of repeated exposure to antigen, they are not exhausted and indeed retain their functionality over time. These features are highly relevant to the development of new vaccines eliciting sustained effective T cell memory responses for certain chronic viral infections.

Although MCMV is a good model to study CMV infection, there are limitations in examining the mechanisms of memory inflation, because it is a complex system, both virologically with its long-term low-grade persistence, its latency and stochastic reactivation at diverse sites, as well as immunologically, with multiple immunologic mechanisms required to establish and maintain control, and a wide range of $CD8^+$ T cell epitopes. Thus, to further understand the mechanism of $CD8^+$ T cell memory inflation, which is still poorly understood, we developed a simpler and more tractable model using Ad-LacZ. In this study, we showed that Ad-LacZ, a non-replicating adenovirus vector, induced a robust inflating $CD8^+$ T cell population against the βgal_{96}-epitope and a conventional $CD8^+$ memory T cell response to the βgal_{497}-epitope after a single i.v. injection in C57BL/6 mice. $CD8^+$ T cell memory inflation after Ad-LacZ immunization revealed strong resemblance to that seen in MCMV infection, providing us with a novel, robust model for memory inflation that is internally controlled and allows dissection of the mechanism underpinning $CD8^+$ T cell memory inflation. These data further support the idea that memory inflation is a

stereotypical pathway of the immunologic memory rather than a unique feature of CMVs, and is consistent with observational data other viral infections (17-20).

In the present study we demonstrated that βgal_{96}-specific inflating $CD8^+$ T cells were polyfunctional and cytotoxic. Although their effector-memory phenotype is consistent with repeated antigen encounter, they were not exhausted compared to $CD8^+$ T cells in other chronic viral infections (particularly LCMV in the mouse but also HIV, HCV and HBV). We further showed, that after i.v. immunization with Ad-LacZ, viral genome was still found at very late timepoints and antigen was expressed and presented at very low levels (Figure 6A-D). These findings imply that long-term maintenance of specific $CD8^+$ T cells after rec-Ad immunization depends on the very low levels of transcriptionally active adenovirus vector genomes. In the context of vaccines this suggests that persisting low-level antigen might be beneficial resulting in the maintenance of functional T_{EM} in the periphery, at sites of pathogen entry.

Using different routes of injection, we observed that memory inflation after Ad-LacZ immunization is not restricted to the i.v. route, but is also seen after i.d. immunization. S.c. immunization induced a variant pattern of a βgal_{96}-specific $CD8^+$ T cell response, which was reduced in magnitude and did not increase but was nevertheless sustained over time (Figure 2, Supplementary Figure 2). Importantly, although only i.v., i.d. and i.m. routes gave strictly-defined inflation, in terms of increasing frequencies of βgal_{96}-specific cells (Day 100/21 ratio >1), an identical effector-memory phenotype was observed in all cases i.e. after i.v., i.d., s.c. and i.m. immunization. This illustrates that while the magnitude and kinetics of the βgal_{96}-specific $CD8^+$ T cell memory response are dependent on the route of immunization, the phenotype is not (Figure 2, Supplementary Figure 2). Two factors are likely to influence these phenomena – firstly, antigen dose and secondly antigen distribution, the latter reflected in the APC involved in priming and in memory maintenance. Previous work by other groups (26, 27) demonstrated that the route and dose of adenovirus-based vaccine delivery impacts on distribution of the virus and thus expansion and trafficking of vaccine-elicited $CD8^+$ T cells. In such experiments, differences in antigen dissemination would readily account for the reduced overall magnitude of the $CD8^+$ T cell response with the non-i.v. compared to the i.v. routes. The distinctive phenotype of inflating populations is, however, shared between populations regardless of the route or magnitude – likewise, regardless of route there are marked differences in phenotype between the inflating and non-inflating epitopes, which emerge over time. The nature of the APC involved in antigen-presentation during the memory phase is discussed further below, but it therefore appears that this APC must be accessible to the inflating memory pool regardless of the route of immunization.

In this study we also showed that the βgal_{96}-specific $CD8^+$ T cell response was significantly reduced in MHC-II-deficient mice. However, unlike the situation with different routes, βgal_{96}-specific $CD8^+$ T cells in MHC-II-KO mice also displayed an altered phenotype compared to the standard i.v inoculation in WT mice; overall this could be summarized as skewed towards a T_{CM}-phenotype rather than the T_{EM}-phenotype typically seen (data not shown). Interestingly although $CD8^+$ T cell expansion was significantly reduced, on day 100 following immunization, βgal_{96}-specific $CD8^+$ T cells were nevertheless still present in blood, liver, lung and spleen (Figure 7A, B). Thus $CD4^+$ T cell help is clearly essential both for the initial priming of βgal_{96}-specific $CD8^+$ T cells and the evolution of an effector-memory phenotype. However, for the maintenance of these cells in the memory phase, $CD4^+$ T cell help might be dispensable. This theory is supported by findings exploiting other recombinant adenovirus vectors (rAdVs) (42, 46). $CD4^+$ T cell help is likely required during memory inflation in MCMV infection, although the situation is more complex (16, 45). In a model where MCMV reactivation was controlled by injection of an antiviral drug, $CD4^+$ T

cell help appears necessary; if viral reactivation is not controlled, $CD4^+$ T cell help can partially be compensated and less impact on memory inflation was observed (16). Overall, in a setting without viral replication, memory inflation is dependent on $CD4^+$ T cell help; however, further experiments are required to determine at what stage such help is critical.

We demonstrated that $CD8^+$ T cell memory inflation in this system was not dependent on viral reactivation and replication (Figure 6). Similar findings were reported for MCMV infection (15, 16), although the levels of inflation seen in these studies were relatively limited. In our model, substantial memory inflation and conventional memory are both induced with a widely used non-replicating adenovirus vector. Prolonged $CD8^+$ T cell responses for several weeks after adenoviral vector immunization has been described previously, followed by contraction, (21, 25, 29-31, 46, 47) although robust $CD8^+$ T cell memory inflation sustained over many months has not been observed. Previous studies have indicated that prolonged $CD8^+$ T cell responses depended on low levels of antigen (30, 31). Interestingly in such models, specific $CD8^+$ T cells become antigen-independent, as shown using a doxycycline-regulated adenovirus vector transgenic for SIINFEKL (30).

We further exploited the model to analyze the dependence of memory inflation after Ad-LacZ immunization on processing via immunoproteasomes. Immunization of LMP7-KO mice, revealed a comparable βgal_{96}-specific $CD8^+$ T cell response to that seen in WT mice. In contrast, the non-inflating βgal_{497}-specific response was completely abolished in LMP7-KO mice (Figure 7D-G). Interestingly, identical findings regarding immunoproteasome-dependency were observed after MCMV-infection (14). Clearly, in both settings, processing of inflating epitopes was not dependent on immunoproteasomes (Figure 7D,E, (14)). Because of the non-inflammatory environment in the Ad-LacZ model, as well as in MCMV latency, these combined data strongly suggest that processing of inflating epitopes depends on constitutively expressed proteasomes. Constitutively expressed proteasomes can be found in hematopoietic APCs (hAPCs) as well as in non-hematopoietic APCs (nhAPCs). Recent data from studies with MCMV demonstrated that hAPC primed MCMV-specific $CD8^+$ T cells but were not sufficient for driving memory inflation (48) and that non-hematopoietic cells, likely in the LNs, were responsible for driving memory inflation in MCMV infection (41). Similar data were obtained with a rAdV (29). Thus, our data from LMP7-KO mice support the theory of APC from a non-hematopoietic origin being responsible for prolonged antigen presentation resulting in memory inflation.

Which nhAPCs might be responsible - and where - remains to be defined. It has been shown that the major reservoir of MCMV latent genomes are cells of non-hematopoietic (nh) origin such as sinusoidal lining cells of the spleen (49), liver sinusoidal endothelial cells (LSECs) (50) or $CD11b^-$ $CX3CR1^-$ nh cells in the lung (51). After i.v. Ad-LacZ immunization, most of the viral genome is found in spleen, liver and lung. We directly tested the role of splenic antigen by repeating the experiments in splenectomized mice, and found no effect of splenectomy (Supplementary Figure 4). Since memory inflation is not impaired in the absence of a spleen, this suggests the liver and/or the lung are the main sites of antigen presentation. Our quantitative realtime PCR results for LacZ DNA as well as the proliferation behavior of adoptively transferred TCR transgenic $CD8^+$ T cells further support this idea. Here, directly infected EC or stromal cells could be potential APC since evidence suggests direct presentation during memory inflation (41). However, whether this is true after i.v. Ad-LacZ immunization still requires investigation. Regardless of the cell-type, it remains unclear how antigen-expressing cells can persist in the presence of specific $CD8^+$ T cell immunity, although potentially such pools may simply decline very slowly.

The observation that βgal_{96}-specific $CD8^+$ T cells are not exhausted and located at a high frequency in peripheral organs, renders them to a very desirable cell population for T cell

inducing vaccines. In this context, effector-memory T cells have been shown to respond rapidly to invasive and proliferating pathogens and were highly protective in epithelial challenges (5). The very high frequencies of specific effector cells at the site of infection might compensate for the reduced proliferative and functional capacity of T_{EM}, compared to T_{CM} (52, 53). Specifically, for chronic HBV and HCV infection and Mycobacterium tuberculosis, where a high number of functional $CD8^+$ T cells in the liver or lung is required to eliminate the pathogen, such a vaccine strategy would be of major importance. Interestingly, recent studies using i.m. vaccination with recombinant adenoviral vector to induce T cell responses against hepatitis C virus revealed a distinct phenotype with sustained development of effector memory $CD8^+$ T cell populations (CD45RA+/−, CCR7−) (21), showing some features of this phenomenon may be already embedded in current vaccine programs.

To further exploit this however, we should first identify and then target the APC population(s) responsible for antigen processing and presentation during the memory phase. DC-based strategies may in theory run the risk of selecting $CD8^+$ T cell populations, which, after the first phase, contract to a low-level memory population of a T_{CM} phenotype. Secondly, we should further dissect the molecular mechanisms underpinning the evolution of inflationary $CD8^+$ T cell responses to promote this pathway of memory development. Thirdly, we should optimize methods to identify and/or generate inflating epitopes from longer proteins. Clearly memory inflation depends not only on the processing of the peptide but other features of the vector. But given the data on immunoproteasome independence, defining the rules governing the relevant cleavage of inflating versus non-inflating peptides should be a priority for future vaccine design. Inflating/immunoproteasome-independent epitopes and non-inflating/immunoproteasome-dependent epitopes could both be included in order to induce long-lived and functional $CD8^+$ T cell effector and central memory populations.

Overall we propose, that although MCMV infection and Ad-LacZ immunization are two completely distinct settings, the mechanism for $CD8^+$ T cell memory inflation is comparable in the two models. Together with findings from studies with other rec-AdV and from MCMV infection we suggest that $CD8^+$ T cell memory inflation is a distinct, evolutionarily conserved, stereotypical memory response, observed after different routes of exposure to diverse vectors. This response depends at least initially on $CD4^+$ T cell help and may depend on presentation of antigen during the memory phase by unconventional (non-DC) APCs, lacking immunoproteasomes.

Rec-AdVs are well characterized and generally easy to manipulate. They transduce a variety of cells, but the vector genome does not integrate and their safety is well established (25). In contrast, CMV would need substantial further work on its use as a vector regarding the safety and efficiency profile. Therefore, the Ad-LacZ-model not only facilitates further studies on $CD8^+$ T cell memory inflation, but also enables direct implications, because of adenoviruses wide potential as vaccine vectors. This convergence of a window on an emerging and tractable area of immunobiology with a technology which forms the basis for many major vaccine programs means the model presented here should be of general value and the implications of the results obtained of broad relevance in future.

Supplementary Material

Refer to Web version on PubMed Central for supplementary material.

Acknowledgments

We would like to thank Dr Chris Norbury, Dr Kevin Maloy and Dr Marcus Groettrup for providing mice (as mentioned in the material and methods section), Chris Willberg for technical support and Peter Beverley for the critical discussion of the results.

References

1. O'Hara GA, Welten SP, Klenerman P, Arens R. Memory T cell inflation: understanding cause and effect. Trends in immunology. 2012; 33:84–90. [PubMed: 22222196]
2. Moskophidis D, Lechner F, Pircher H, Zinkernagel RM. Virus persistence in acutely infected immunocompetent mice by exhaustion of antiviral cytotoxic effector T cells. Nature. 1993; 362:758–761. [PubMed: 8469287]
3. Wherry EJ. T cell exhaustion. Nature immunology. 2011; 12:492–499. [PubMed: 21739672]
4. Karrer U, Sierro S, Wagner M, Oxenius A, Hengel H, Koszinowski UH, Phillips RE, Klenerman P. Memory inflation: continuous accumulation of antiviral CD8+ T cells over time. J.Immunol. 2003; 170:2022–2029. [PubMed: 12574372]
5. Hansen SG, Ford JC, Lewis MS, Ventura AB, Hughes CM, Coyne-Johnson L, Whizin N, Oswald K, Shoemaker R, Swanson T, Legasse AW, Chiuchiolo MJ, Parks CL, Axthelm MK, Nelson JA, Jarvis MA, Piatak M Jr. Lifson JD, Picker LJ. Profound early control of highly pathogenic SIV by an effector memory T-cell vaccine. Nature. 2011; 473:523–527. [PubMed: 21562493]
6. Holtappels R, Pahl-Seibert MF, Thomas D, Reddehase MJ. Enrichment of immediate-early 1 (m123/pp89) peptide-specific CD8 T cells in a pulmonary CD62L(lo) memory-effector cell pool during latent murine cytomegalovirus infection of the lungs. J.Virol. 2000; 74:11495–11503. [PubMed: 11090146]
7. Komatsu H, Sierro S, Cuero V, Klenerman P. Population analysis of antiviral T cell responses using MHC class I-peptide tetramers. Clin.Exp.Immunol. 2003; 134:9–12. [PubMed: 12974748]
8. Northfield J, Lucas M, Jones H, Young NT, Klenerman P. Does memory improve with age? CD85j (ILT-2/LIR-1) expression on CD8 T cells correlates with 'memory inflation' in human cytomegalovirus infection. Immunol.Cell Biol. 2005; 83:182–188. [PubMed: 15748215]
9. Snyder CM, Cho KS, Bonnett EL, van Dommelen S, Shellam GR, Hill AB. Memory inflation during chronic viral infection is maintained by continuous production of short-lived, functional T cells. Immunity. 2008; 29:650–659. [PubMed: 18957267]
10. Sierro S, Rothkopf R, Klenerman P. Evolution of diverse antiviral CD8+ T cell populations after murine cytomegalovirus infection. Eur.J.Immunol. 2005; 35:1113–1123. [PubMed: 15756645]
11. Sylwester AW, Mitchell BL, Edgar JB, Taormina C, Pelte C, Ruchti F, Sleath PR, Grabstein KH, Hosken NA, Kern F, Nelson JA, Picker LJ. Broadly targeted human cytomegalovirus-specific CD4+ and CD8+ T cells dominate the memory compartments of exposed subjects. J.Exp.Med. 2005; 202:673–685. [PubMed: 16147978]
12. Munks MW, Cho KS, Pinto AK, Sierro S, Klenerman P, Hill AB. Four distinct patterns of memory CD8 T cell responses to chronic murine cytomegalovirus infection. J.Immunol. 2006; 177:450–458. [PubMed: 16785542]
13. Munks MW, Gold MC, Zajac AL, Doom CM, Morello CS, Spector DH, Hill AB. Genome-wide analysis reveals a highly diverse CD8 T cell response to murine cytomegalovirus. J.Immunol. 2006; 176:3760–3766. [PubMed: 16517745]
14. Hutchinson S, Sims S, O'Hara G, Silk J, Gileadi U, Cerundolo V, Klenerman P. A dominant role for the immunoproteasome in CD8+ T cell responses to murine cytomegalovirus. PloS one. 2011; 6:e14646. [PubMed: 21304910]
15. Snyder CM, Cho KS, Bonnett EL, Allan JE, Hill AB. Sustained CD8+ T cell memory inflation after infection with a single-cycle cytomegalovirus. PLoS pathogens. 2011; 7:e1002295. [PubMed: 21998590]
16. Walton SM, Torti N, Mandaric S, Oxenius A. T-cell help permits memory CD8(+) T-cell inflation during cytomegalovirus latency. European journal of immunology. 2011; 41:2248–2259. [PubMed: 21590767]

17. Isa A, Kasprowicz V, Norbeck O, Loughry A, Jeffery K, Broliden K, Klenerman P, Tolfvenstam T, Bowness P. Prolonged activation of virus-specific CD8+T cells after acute B19 infection. PLoS medicine. 2005; 2:e343. [PubMed: 16253012]
18. Lang A, Brien JD, Nikolich-Zugich J. Inflation and long-term maintenance of CD8 T cells responding to a latent herpesvirus depend upon establishment of latency and presence of viral antigens. Journal of immunology. 2009; 183:8077–8087.
19. Simmons R, Sharp C, Sims S, Kloverpris H, Goulder P, Simmonds P, Bowness P, Klenerman P. High frequency, sustained T cell responses to PARV4 suggest viral persistence in vivo. The Journal of infectious diseases. 2011; 203:1378–1387. [PubMed: 21502079]
20. Swanson PA 2nd, Hofstetter AR, Wilson JJ, Lukacher AE. Cutting edge: shift in antigen dependence by an antiviral MHC class Ib-restricted CD8 T cell response during persistent viral infection. Journal of immunology. 2009; 182:5198–5202.
21. Barnes E, Folgori A, Capone S, Swadling L, Aston S, Kurioka A, Meyer J, Huddart R, Smith K, Townsend R, Brown A, Antrobus R, Ammendola V, Naddeo M, O'Hara G, Willberg C, Harrison A, Grazioli F, Esposito ML, Siani L, Traboni C, Oo Y, Adams D, Hill A, Colloca S, Nicosia A, Cortese R, Klenerman P. Novel adenovirus-based vaccines induce broad and sustained T cell responses to HCV in man. Science translational medicine. 2012; 4:115ra111.
22. Singh S, Toro H, Tang DC, Briles WE, Yates LM, Kopulos RT, Collisson EW. Non-replicating adenovirus vectors expressing avian influenza virus hemagglutinin and nucleocapsid proteins induce chicken specific effector, memory and effector memory CD8(+) T lymphocytes. Virology. 2010; 405:62–69. [PubMed: 20557918]
23. Zhang HG, Wang YM, Xie JF, Liang X, Hsu HC, Zhang X, Douglas J, Curiel DT, Mountz JD. Recombinant adenovirus expressing adeno-associated virus cap and rep proteins supports production of high-titer recombinant adeno-associated virus. Gene Ther. 2001; 8:704–712. [PubMed: 11406765]
24. Ziegler RJ, Li C, Cherry M, Zhu Y, Hempel D, van Rooijen N, Ioannou YA, Desnick RJ, Goldberg MA, Yew NS, Cheng SH. Correction of the nonlinear dose response improves the viability of adenoviral vectors for gene therapy of Fabry disease. Hum.Gene Ther. 2002; 13:935–945. [PubMed: 12031126]
25. Bassett JD, Swift SL, Bramson JL. Optimizing vaccine-induced CD8(+) T-cell immunity: focus on recombinant adenovirus vectors. Expert review of vaccines. 2011; 10:1307–1319. [PubMed: 21919620]
26. Holst PJ, Orskov C, Thomsen AR, Christensen JP. Quality of the transgene-specific CD8+ T cell response induced by adenoviral vector immunization is critically influenced by virus dose and route of vaccination. Journal of immunology. 2010; 184:4431–4439.
27. Kaufman DR, Bivas-Benita M, Simmons NL, Miller D, Barouch DH. Route of adenovirus-based HIV-1 vaccine delivery impacts the phenotype and trafficking of vaccine-elicited CD8+ T lymphocytes. Journal of virology. 2010; 84:5986–5996. [PubMed: 20357087]
28. Krebs P, Scandella E, Odermatt B, Ludewig B. Rapid functional exhaustion and deletion of CTL following immunization with recombinant adenovirus. J.Immunol. 2005; 174:4559–4566. [PubMed: 15814677]
29. Bassett JD, Yang TC, Bernard D, Millar JB, Swift SL, McGray AJ, VanSeggelen H, Boudreau JE, Finn JD, Parsons R, Evelegh C, Damjanovic D, Grinshtein N, Divangahi M, Zhang L, Xing Z, Wan Y, Bramson JL. CD8+ T-cell expansion and maintenance after recombinant adenovirus immunization rely upon cooperation between hematopoietic and nonhematopoietic antigen-presenting cells. Blood. 2011; 117:1146–1155. [PubMed: 21088134]
30. Finn JD, Bassett J, Millar JB, Grinshtein N, Yang TC, Parsons R, Evelegh C, Wan Y, Parks RJ, Bramson JL. Persistence of transgene expression influences CD8+ T-cell expansion and maintenance following immunization with recombinant adenovirus. Journal of virology. 2009; 83:12027–12036. [PubMed: 19759135]
31. Tatsis N, Fitzgerald JC, Reyes-Sandoval A, Harris-McCoy KC, Hensley SE, Zhou D, Lin SW, Bian A, Xiang ZQ, Iparraguirre A, Lopez-Camacho C, Wherry EJ, Ertl HC. Adenoviral vectors persist in vivo and maintain activated CD8+ T cells: implications for their use as vaccines. Blood. 2007; 110:1916–1923. [PubMed: 17510320]

32. Manning WC, Mocarski ES. Insertional mutagenesis of the murine cytomegalovirus genome: one prominent alpha gene (ie2) is dispensable for growth. Virology. 1988; 167:477–484. [PubMed: 2849236]
33. Ludewig B, Ochsenbein AF, Odermatt B, Paulin D, Hengartner H, Zinkernagel RM. Immunotherapy with dendritic cells directed against tumor antigens shared with normal host cells results in severe autoimmune disease. The Journal of experimental medicine. 2000; 191:795–804. [PubMed: 10704461]
34. Kontgen F, Suss G, Stewart C, Steinmetz M, Bluethmann H. Targeted disruption of the MHC class II Aa gene in C57BL/6 mice. International immunology. 1993; 5:957–964. [PubMed: 8398989]
35. Bolinger B, Krebs P, Tian Y, Engeler D, Scandella E, Miller S, Palmer DC, Restifo NP, Clavien PA, Ludewig B. Immunologic ignorance of vascular endothelial cells expressing minor histocompatibility antigen. Blood. 2008; 111:4588–4595. [PubMed: 18195091]
36. Fehling HJ, Swat W, Laplace C, Kuhn R, Rajewsky K, Muller U, von Boehmer H. MHC class I expression in mice lacking the proteasome subunit LMP-7. Science. 1994; 265:1234–1237. [PubMed: 8066463]
37. Overwijk WW, Surman DR, Tsung K, Restifo NP. Identification of a Kb-restricted CTL epitope of beta-galactosidase: potential use in development of immunization protocols for “self” antigens. Methods. 1997; 12:117–123. [PubMed: 9184376]
38. Oukka M, Cohen-Tannoudji M, Tanaka Y, Babinet C, Kosmatopoulos K. Medullary thymic epithelial cells induce tolerance to intracellular proteins. J.Immunol. 1996; 156:968–975. [PubMed: 8558024]
39. Gold MC, Munks MW, Wagner M, Koszinowski UH, Hill AB, Fling SP. The murine cytomegalovirus immunomodulatory gene m152 prevents recognition of infected cells by M45-specific CTL but does not alter the immunodominance of the M45-specific CD8 T cell response in vivo. J.Immunol. 2002; 169:359–365. [PubMed: 12077265]
40. Altman JD, Moss PAH, Goulder PJR, Barouch DH, McHeyzer-Williams MG, Bell JI, McMichael AJ, Davis MM. Phenotypic analysis of antigen-specific T lymphocytes. Science. 1996; 274:94–96. [PubMed: 8810254]
41. Torti N, Walton SM, Brocker T, Rulicke T, Oxenius A. Non-hematopoietic cells in lymph nodes drive memory CD8 T cell inflation during murine cytomegalovirus infection. PLoS pathogens. 2011; 7:e1002313. [PubMed: 22046127]
42. Yang TC, Millar J, Groves T, Zhou W, Grinshtein N, Parsons R, Evelegh C, Xing Z, Wan Y, Bramson J. On the role of CD4+ T cells in the CD8+ T-cell response elicited by recombinant adenovirus vaccines. Molecular therapy: the journal of the American Society of Gene Therapy. 2007; 15:997–1006. [PubMed: 17375073]
43. Harty JT, Badovinac VP. Shaping and reshaping CD8+ T-cell memory. Nature reviews. Immunology. 2008; 8:107–119.
44. Wiesel M, Walton S, Richter K, Oxenius A. Virus-specific CD8 T cells: activation, differentiation and memory formation. APMIS: acta pathologica, microbiologica, et immunologica Scandinavica. 2009; 117:356–381.
45. Snyder CM, Loewendorf A, Bonnett EL, Croft M, Benedict CA, Hill AB. CD4+ T cell help has an epitope-dependent impact on CD8+ T cell memory inflation during murine cytomegalovirus infection. Journal of immunology. 2009; 183:3932–3941.
46. Holst PJ, Bartholdy C, Stryhn A, Thomsen AR, Christensen JP. Rapid and sustained CD4(+) T-cell-independent immunity from adenovirus-encoded vaccine antigens. The Journal of general virology. 2007; 88:1708–1716. [PubMed: 17485530]
47. Yang TC, Millar JB, Grinshtein N, Bassett J, Finn J, Bramson JL. T-cell immunity generated by recombinant adenovirus vaccines. Expert review of vaccines. 2007; 6:347–356. [PubMed: 17542750]
48. Seckert CK, Schader SI, Ebert S, Thomas D, Freitag K, Renzaho A, Podlech J, Reddehase MJ, Holtappels R. Antigen-presenting cells of haematopoietic origin prime cytomegalovirus-specific CD8 T-cells but are not sufficient for driving memory inflation during viral latency. The Journal of general virology. 2011; 92:1994–2005. [PubMed: 21632567]

49. Mercer JA, Wiley CA, Spector DH. Pathogenesis of murine cytomegalovirus infection: identification of infected cells in the spleen during acute and latent infections. Journal of virology. 1988; 62:987–997. [PubMed: 2828694]

50. Seckert CK, Renzaho A, Tervo HM, Krause C, Deegen P, Kuhnapfel B, Reddehase MJ, Grzimek NK. Liver sinusoidal endothelial cells are a site of murine cytomegalovirus latency and reactivation. Journal of virology. 2009; 83:8869–8884. [PubMed: 19535440]

51. Marquardt A, Halle S, Seckert CK, Lemmermann NA, Veres TZ, Braun A, Maus UA, Forster R, Reddehase MJ, Messerle M, Busche A. Single cell detection of latent cytomegalovirus reactivation in host tissue. The Journal of general virology. 2011; 92:1279–1291. [PubMed: 21325477]

52. Kaech SM, Wherry EJ, Ahmed R. Effector and memory T-cell differentiation: implications for vaccine development. Nature reviews. Immunology. 2002; 2:251–262.

53. Wherry EJ, Teichgraber V, Becker TC, Masopust D, Kaech SM, Antia R, von Andrian UH, Ahmed R. Lineage relationship and protective immunity of memory CD8 T cell subsets. Nature immunology. 2003; 4:225–234. [PubMed: 12563257]

Europe PMC Funders Author Manuscripts

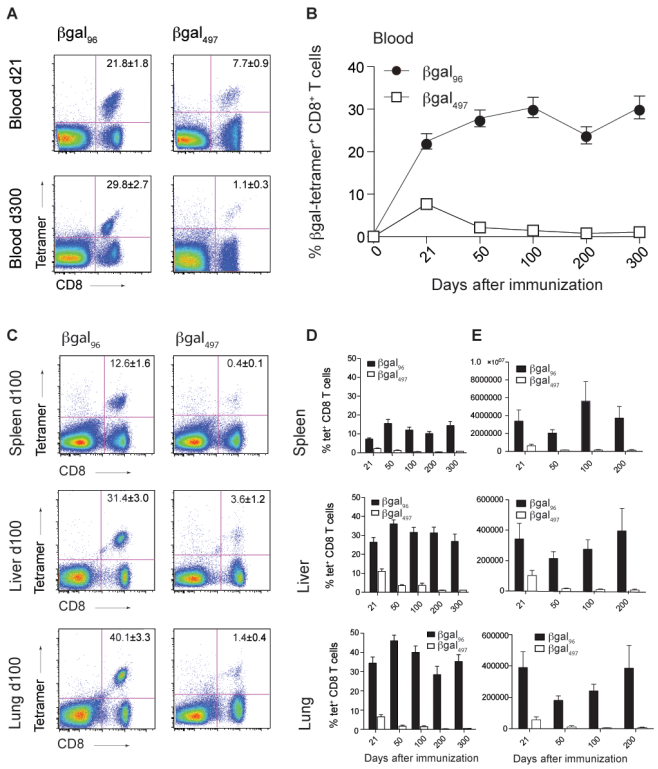

Figure 1. A single dose of Ad-LacZ is sufficient to induce CD8$^+$ T cell memory inflation

C57BL/6 (B6) mice were immunized intravenously (i.v.) with 2×10^9 pfu Ad-LacZ. Tetramer analysis for the indicated βgal-epitopes was performed on day 21, 50, 100, 200 and 300 after immunization. (A) Tetramer staining for βgal_{96}- and βgal_{497}-specific CD8$^+$ lymphocytes on d21 and 300 in blood, gated on live lymphocytes. (B) Expansion of βgal_{96}- (black circles) and βgal_{497}-specific (white squares) CD8$^+$ T cells in blood. (C) Tetramer staining for βgal_{96}- and βgal_{497}-specific CD8$^+$ lymphocytes on d100 in spleen, liver and lung. (D) Tetramer analysis for lymphocytes from spleen, liver and lung on days 21, 50, 100, 200 and 300. Mean percentage of tetramer-positive cells within the CD8$^+$ T cell compartment are indicated (±SEM; blood d21 n=17, d50 n=21, d100 n=15, d200 n=12, d300 n=12; spleen d21 n=16, d50 n=15, d100 n=8, d200 n=9, d300 n=10; liver and lung d21 n=13, d50 n=17, d100 n=8, d200 n=9, d300 n=9). (E) Total counts of βgal_{96}- and βgal_{497}-specific CD8$^+$ lymphocytes in spleen, liver and lung on days 21, 50, 100 and 200 after immunization. Mean of total numbers of tetramer-positive cells within the CD8$^+$ T cell compartment are indicated (±SEM; spleen d21 n=16, d50 n=13 d100 n=8, d200 n=6, liver and lung d21 n=12, d50 n=12, d100 n=11, d200 n=6). Each experiment was at least repeated once.

Europe PMC Funders Author Manuscripts

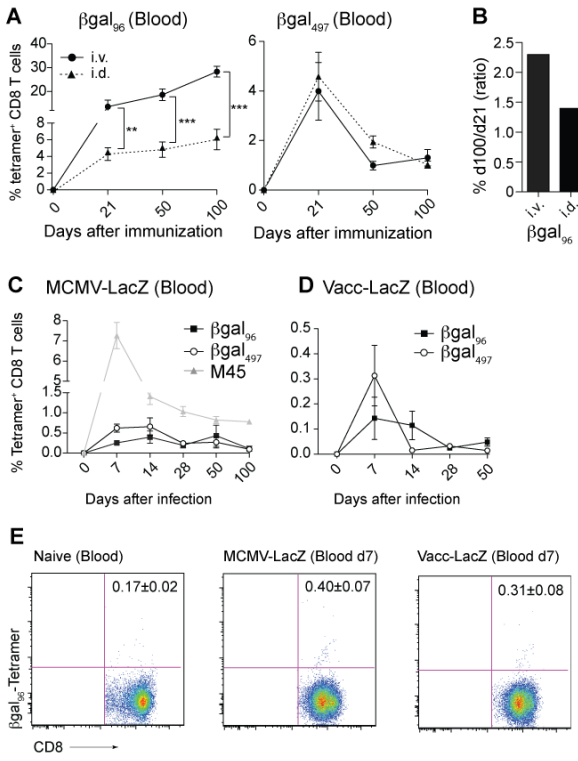

Figure 2. βgal_{96}-specific $CD8^+$ T memory inflation is not restricted to the i.v. route, but is unique to Ad-LacZ

(A) B6 mice were immunized i.v. (black circles) or i.d. (dotted line, black triangles) with 2×10^9 pfu Ad-LacZ and expansion of βgal_{96}-$tetramer^+$ $CD8^+$ T cells was measured. The magnitude of the βgal_{96}-specific $CD8^+$ T cell response is significantly reduced after i.d. immunization compared to i.v. immunization, at all timepoints. Mean percentage of tetramer-positive cells within the $CD8^+$ compartment is indicated (±SEM; blood d21 n= 7, d50 n=7, d100 n=7; data from two independently performed experiments). (B) Inflationary potential expressed by the ratio of percentage of tetramer-positive $CD8^+$ T cells from day 100 to day 21 in C57BL/6 mice after i.v. and i.d. immunization for both βgal epitopes. (C) B6 mice were i.v. infected with 2×10^6 pfu MCMV-LacZ and expansion of βgal_{96} - (black squares), βgal_{497}- (white circles) and M45 (=MCMV-specific control, grey triangles) $tetramer^+$ $CD8^+$ T cells was measured with flow cytometry. Mean percentages of tetramer-positive cells within the $CD8^+$ compartment are indicated (±SEM; d7 n=7-9, d14 n=7-10, d28 n= 7, d50 n=7-10, d100 n=6; data from two independently performed experiments). (D) B6 mice were infected i.p. with 2×10^6 pfu Vaccinia-LacZ (Vacc-LacZ) and expansion of βgal_{96}- (black square) and βgal_{497}- (white circle) $tetramer^+$ $CD8^+$ T cells was measured with flow cytometry. Mean percentage of tetramer-positive cells within the $CD8^+$ compartment is indicated (±SEM; d7 n=7, d14 n=7, d28 n=7, d50 n=7; data from two independently performed experiments). (E) Representing FACS plots for βgal_{96}-specific tetramer staining in naïve (=background) B6 mice and MCMV-LacZ and Vacc-LacZ infected B6 mice on day 7 post infection in blood. Mean percentages of tetramer-positive cells (no background subtracted) within the $CD8^+$ compartment are indicated.

Europe PMC Funders Author Manuscripts

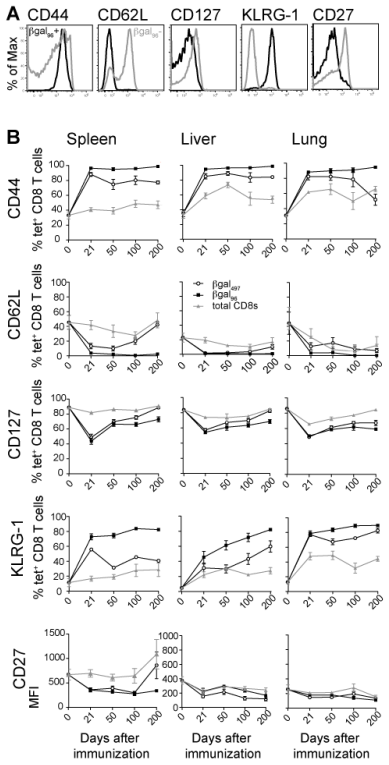

Figure 3. βgal$_{96}$-specific CD8$^+$ T cells display an effector-memory phenotype

(A) Peripheral blood from d100 B6 mice was stained with the βgal$_{96}$ tetramer and antibodies specific for CD8 and the indicated cell surface molecule. The plots shown are gated on tetramer$^+$ CD8$^+$ T cells (black) or tetramer$^-$ CD8$^+$ T cells (grey) from the same sample. (B) Expression of CD44, CD62L, CD127, KLRG-1 and CD27 in βgal$_{96}$ -positive (black squares), βgal$_{497}$-positive (white circles) and total CD8$^+$ T cells (grey triangles) in spleen, liver and lung on different time points after immunization.Mean percentage or MFI respectively of surface molecule positive cells within the tetramer-positive or the CD8$^+$ T cell compartment is indicated (±SEM; blood d21 n=6-13, d50 n= 6-12, d100 n=5-7, d200 n=3-6; spleen d21 n=9-16, d50 n=6-13, d100 n=3-8, d200 n=5-6; liver and lung d21 n=6-10, d50 n=6-9, d100 n=5-8, d200 n=3-6; range indicates the different markers assessed; data from at least two independently performed experiments).

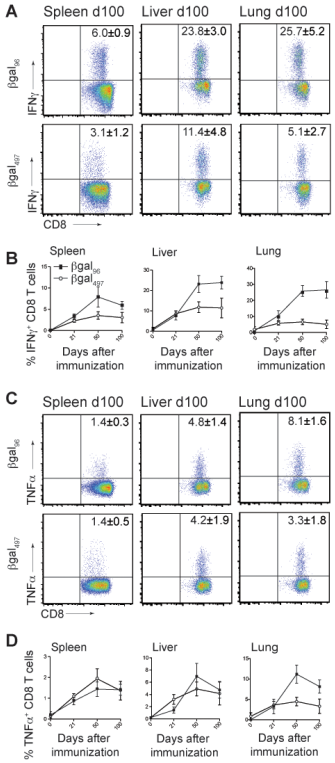

Figure 4. Inflating CD8$^+$ T cells are strong IFNγ and TNFα producers

C57BL/6 mice were immunized with 2×10^9 pfu Ad-LacZ i.v. and intracellular cytokine production assay for IFNγ (A, B) and TNFα (C,D) in the presence of the βgal_{96} or βgal_{497} peptide was performed. (A) FACS plots showing IFNγ production after stimulation with βgal_{96} or βgal_{497} peptide on day 100 in spleen, liver and lung, gated on live CD3$^+$CD8$^+$ T lymphocytes. (B) IFNγ production on d21, d50, d100 in spleen, liver and lung. (C) FACS plots showing TNFα production after stimulation with βgal_{96} or βgal_{497} on day 100 in spleen, liver and lung, gated on live CD3$^+$CD8$^+$ T lymphocytes. (D) TNFα production on d21, d50, d100 in spleen, liver and lung. Mean percentages of IFNγ$^+$ respectively TNFα$^+$ cells within the CD3$^+$CD8$^+$ T cell compartment are indicated (±SEM; spleen d21 n=12, d50 n=12, d100 n=11, d200 n=6; liver and lung d21 n=4, d50 n=9, d100 n=4; data from at least two independently performed experiments).

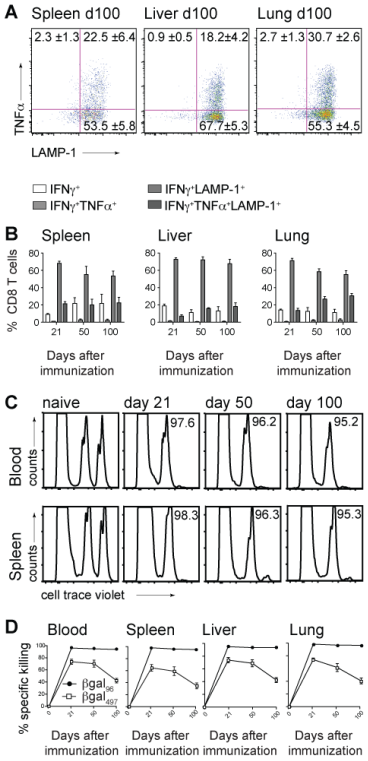

Figure 5. Inflating CD8$^+$ T cells show progressive differentiation towards polyfunctionality and maintain cytotoxicity

B6 mice were immunized with 2×10^9 pfu Ad-LacZ i.v.. (A) FACS plots show TNFα and LAMP-1 expression on day 100 in spleen, liver and lung after in vitro stimulation with the βgal_{96} peptide, gated on live IFNγ$^+$ CD3$^+$CD8$^+$ T lymphocytes. (B) Shows IFNγ single$^+$CD8$^+$ T cells (white bar), IFNγ$^+$TNFα$^+$CD8$^+$ T cells (light grey bars), IFNγ$^+$LAMP1$^+$CD8$^+$ T cells (grey bars) and IFNγ$^+$TNFα$^+$LAMP-1$^+$CD8$^+$ T cells (dark grey bars)within the IFNγ$^+$CD8$^+$ T cell compartment after stimulation with the βgal_{96} peptide in spleen, liver and lung. Mean percentages are indicated (±SEM; spleen d21 n=6, d50 n=6, d100 n=5; liver and lung d21 n=4, d50 n=6, d100 n=7; data from at least two independently performed experiments). (C) βgal_{96}-specific CD8$^+$ T cells kill peptide loaded target cells. Splenocytes from naïve C57BL/6 mice were stained with cellTrace violet, loaded or not with the βgal_{96} peptide and transferred i.v. into naïve B6 mice or B6 mice previously immunized (d21, d50 and d100) with Ad-LacZ. FACS analysis of the surviving donor cells in blood, spleen, liver and lung of recipient mice was performed 12 hours later. FACS plots show the transferred splenocytes (cellTrace violet low=control group; cellTrace violet high=βgal_{96}-pulsed target cells) 12h after transfer in blood and spleen. Target cells have been killed efficiently on d21, d50 and d100. (D) % Specific killing of βgal_{96}- (black circles) or βgal_{497}-(white squares) target cells in blood, spleen, liver and lung was measured 12h after adoptive transfer by FACS analysis in d0, d21, d50 and d100 recipient mice. Mean percentage of specific killing is indicated (±SEM; spleen, blood, liver and lung d21 n=6, d50 n=6, d100 n=8; data from three independently performed experiments).

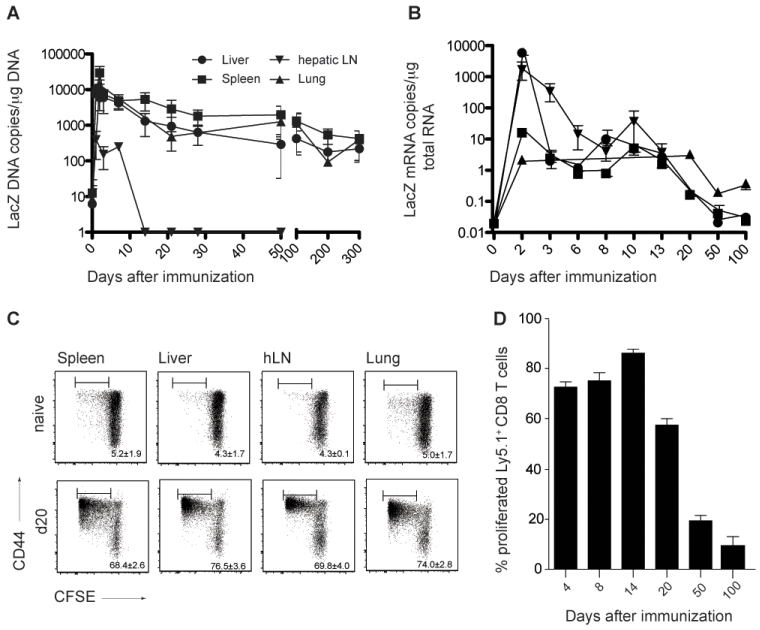

Figure 6. Low-level antigen persistence in Ad-LacZ immunized B6 mice

(A) Viral genome distribution after immunization with Ad-LacZ. LacZ DNA copy numbers per µg total DNA were determined with quantitative realtime PCR on different time points after immunization in liver, lung, spleen and hepatic lymph nodes. Values < 10 copies are detectable but not quantifiable. Pooled data from two independent experiments for each time point are shown (Mean±SEM, liver n=3-12, spleen n=3-12, lung n=3-8, hepatic LN n=3-6). (B) βgal expression after immunization with Ad-LacZ. LacZ mRNA copy numbers per µg total mRNA were determined with quantitative realtime PCR at different timepoints after immunization in liver, lung, spleen and hepatic lymph nodes. mRNA copy numbers < 10 are detectable but not quantifiable. Pooled data from two independent experiments for each time point are shown (Mean±SEM, liver n=3-7, spleen n=3-7, lung n=3-6, hepatic LN n=3-4). (C) Low level antigen persistence after i.v. immunization of B6 mice with Ad-LacZ. CFSE-labeled, βgal_{96}-specific, $Ly5.1^+$ TCR-transgenic $CD8^+$ T cells from Bg1 mice transferred on day 20 after Ad-LacZ immunization proliferated in spleen liver, hepatic LNs and lung 3 days after transfer. The numbers indicate the percentage of proliferated $Ly5.1^+$ $CD8^+$ T cells that are donor derived. Pooled data from two independent experiments for each time point are shown (±SEM, spleen n=4, liver n=4, hLN n=4 lung n=4). (D) Percentage of proliferated $Ly5.1^+$ TCR-transgenic $CD8^+$ T cells in spleen analyzed 3 days after adoptive transfer in mice previously immunized with Ad-LacZ on different time points (d4, d8, d14, d20, d50 and d100). Mean percentage (±SEM n=3-5) is indicated.

Europe PMC Funders Author Manuscripts

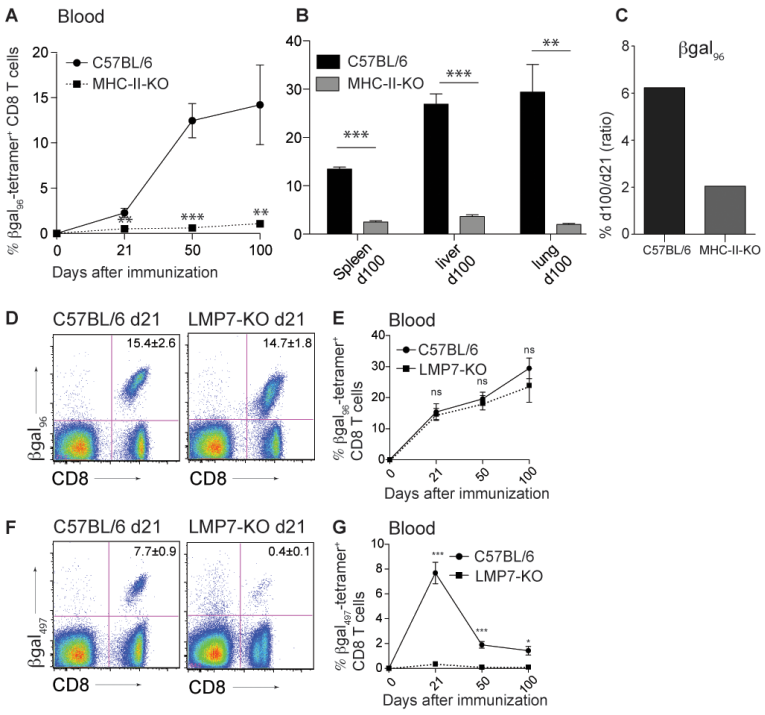

Figure 7. βgal_{96}-specific $CD8^+$ T cell memory inflation critically depends on $CD4^+$ T cell help, but is immunoproteasome-independent

(A, B) No priming and expansion of βgal_{96}-specific $CD8^+$ T cells without CD4 T cell help. B6 and MHC-II-KO mice were immunized intravenously with 2×10^9 pfu Ad-LacZ. Tetramer analysis for βgal_{96}-specific $CD8^+$ T cells was performed on day 21, 50 and 100 after immunization. (A)Expansion of βgal_{96}-specific $CD8^+$ T cells in blood of B6 (black circles) and MHC-II-KO (black squares, dashed line) mice. (B) Tetramer analysis of $CD8^+$ T lymphocytes from spleen, liver and lung of B6 (black bars) and MHC-II-KO (grey bars) mice on day 100 after immunization. Mean percentage of tetramer-positive cells within the $CD8^+$ T cell compartment is indicated (±SEM; blood B6 d21 n=3, d50 n=3, d100 n=3; blood MHC-II-KO d21 n=4, d50 n=4, d100 n=4; spleen, liver and lung B6 d100 n=3; spleen, liver and lung MHC-II-KO d100 n=4; data from a single experiment. This experiment was performed in the animal facility in St. Gallen). (C) Inflationary potential expressed by the ratio of percentage of tetramer-positive $CD8^+$ T cells from day 100 to day 21 in B6 and MHC-II-deficient mice.

(D-G) B6 and LMP7-KO mice were immunized intravenously with 2×10^9 pfu Ad-LacZ. (D)Tetramer staining for βgal_{96}-specific $CD8^+$ T lymphocytes on d21 in blood of C57BL/6 (left) and LMP7-KO (right) mice, gated on live lymphocytes. (E) Expansion of βgal_{96}-specific CD8 T cells in blood of B6 (black circles) and LMP7-KO (black squares, dotted line). (F) Tetramer staining for βgal_{497}-specific $CD8^+$ lymphocytes on d21 in blood of C57BL/6 (left) and LMP7-KO (right) mice, gated on live lymphocytes. (G) Expansion of βgal_{497}-specific $CD8^+$ T cells in blood of B6 (solid/continuous line) and LMP7-KO (dotted line). Mean percentage of tetramer-positive cells within the $CD8^+$ T cell compartment is indicated. Pooled data from two independent experiments for each time point are shown (±SEM; blood B6 d21 n= 10, d50 n=10, d100 n=13; blood LMP7-KO d21 n= 10, d50 n=9, d100 n=5).